Supporting Information for

"Mechanisms of low-frequency oxygen variability in the North Pacific"

Takamitsu Ito [1] **, Matthew C. Long** [2] **, Curtis Deutsch** [3] **, Shoshiro Minobe** [4,5] **and Daoxun Sun** [1]

[1]Georgia Institute of Technology, Atlanta, Georgia, USA.

[2]Climate and Global Dynamics Laboratory, National Center for Atmospheric Research, Boulder, Colorado, USA.

[3]School of Oceanography, University of Washington, Seattle, Washington, USA.

[4]Department of Natural History Sciences, Graduate School of Science, Hokkaido University, Sapporo, Japan.
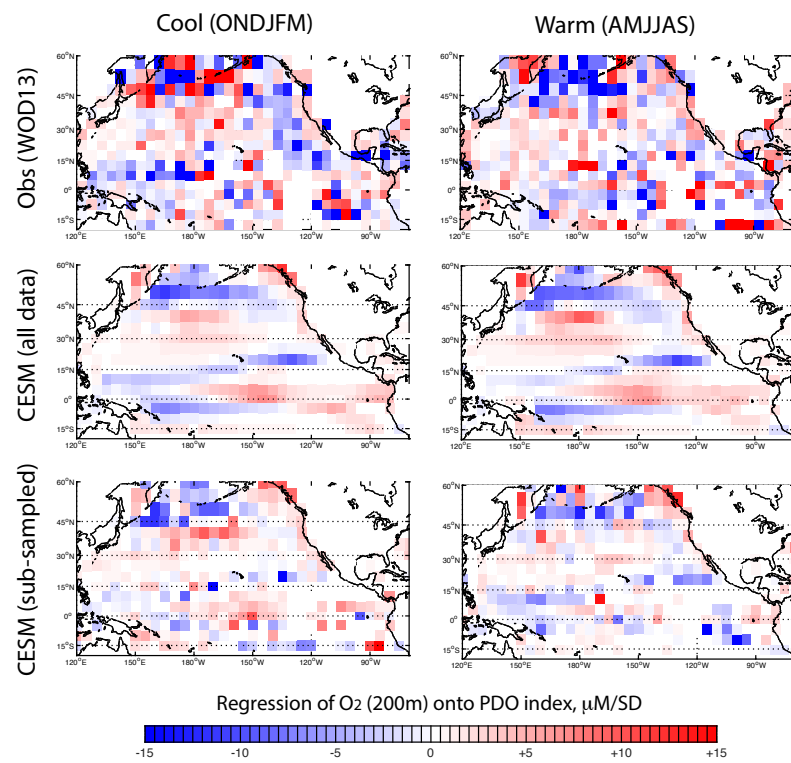
[5]Department of Earth and Planetary Sciences, Faculty of Science, Hokkaido University, Sapporo, Japan.

Contents

1. Figures S1 to S7

Corresponding author: Takamitsu Ito, `taka.ito@eas.gatech.edu`
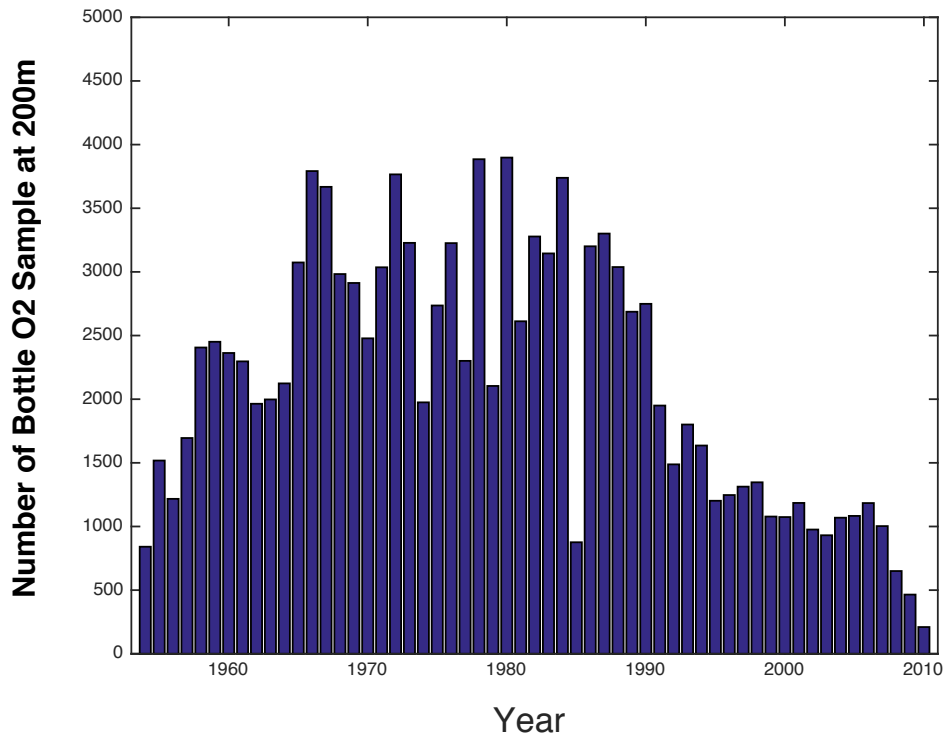
**Figure S1.** Bottle O_2 data count in the Pacific basin between 20° and 60°N in the World Ocean Database 2013.

Figure S2. The observed pattern of O_2 at 200m depth associated with the PDO calculated as a regression coefficient in the units of μM per one standard deviation of the PDO index (μMSD^{-1}). Same as Figure 4 of the main text but the analysis is performed separately for warm and cool seasons.
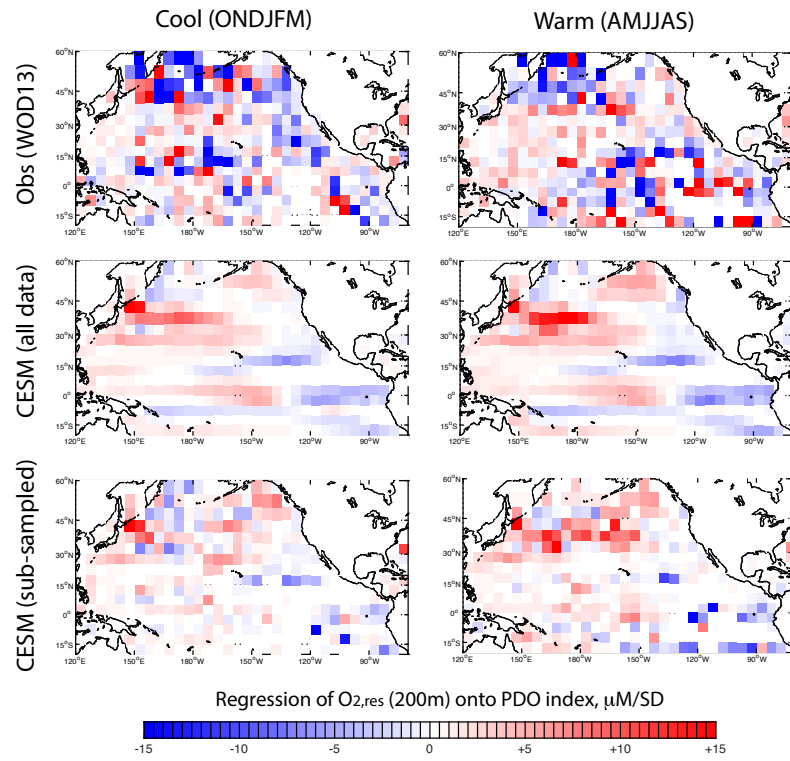
Figure S3. Residual O_2 - PDO relationship as calculated by the regression coeffcient between the $O'_{2,residual}$ and the PDO indices in the units of μMSD^{-1}. Same as Figure 8 of the main text but the analysis is performed separately for warm and cool seasons.
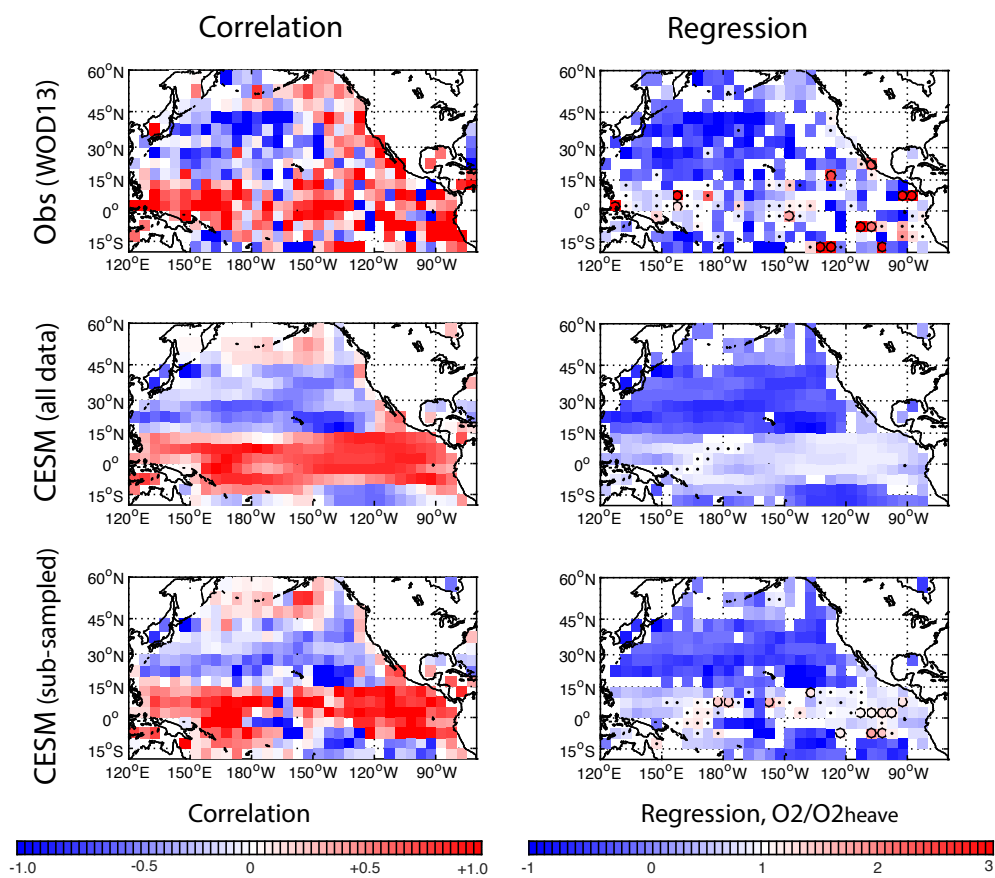
Figure S4. Same as Figure 10 of the main text but for the 100m. (left column) Local correlation coefficients between O_2 and $O_{2,heave}$ at the depth of 100m. (right column) Local regression coefficients. O_2 is regressed onto $O_{2,heave}$ and so its regression coefficients are unitless. (top) Plotted values are from the WOD13 data, (middle) from the full model output, and (bottom) from the subsampled model output.
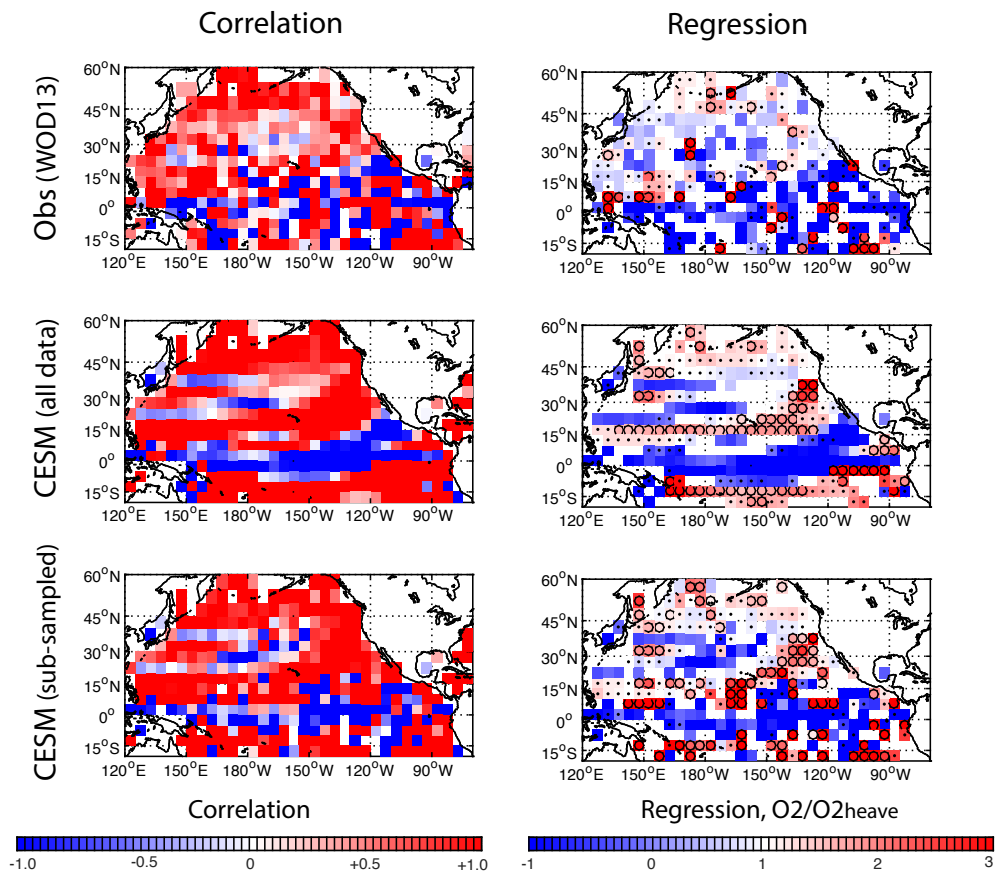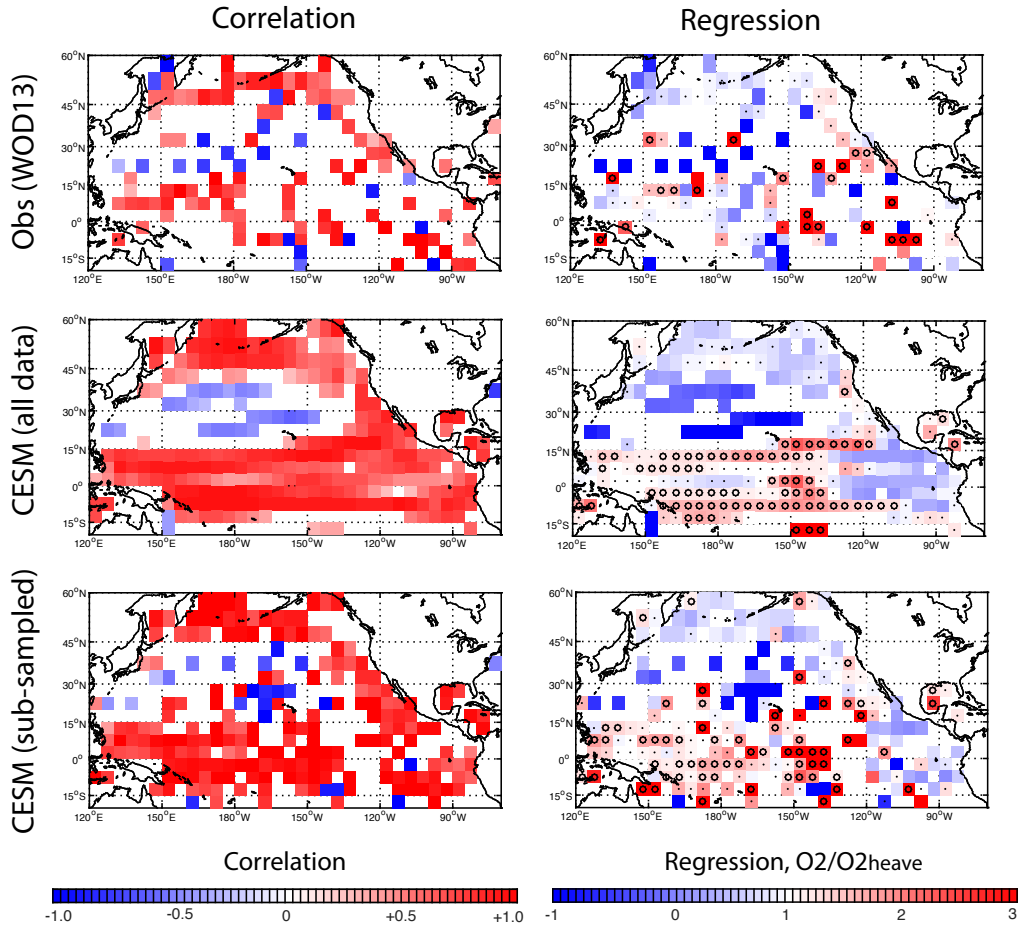
Figure S5. Same as Figure 10 of the main text but for the 400m. (left column) Local correlation coefficients between O_2 and $O_{2,heave}$ at the depth of 400m. (right column) Local regression coefficients. O_2 is regressed onto $O_{2,heave}$ and so its regression coefficients are unitless. (top) Plotted values are from the WOD13 data, (middle) from the full model output, and (bottom) from the subsampled model output.
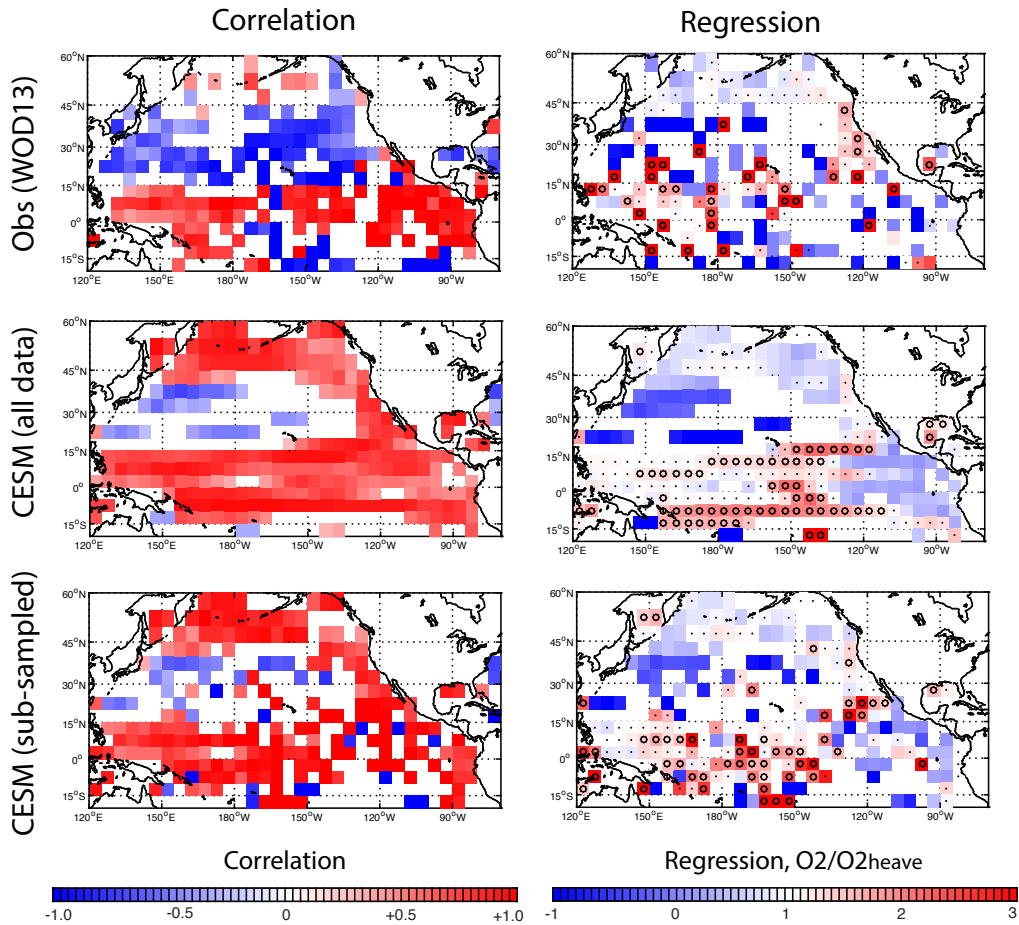
Figure S6. Same as Figure 10 of the main text but for the warm seasons. (left column) Local correlation coefficients between O_2 and $O_{2,heave}$ at the depth of 200m. (right column) Local regression coefficients. O_2 is regressed onto $O_{2,heave}$ and so its regression coefficients are unitless. (top) Plotted values are from the WOD13 data, (middle) from the full model output, and (bottom) from the subsampled model output.

Figure S7. Same as Figure 10 of the main text but for the cool seasons. (left column) Local correlation coefficients between O_2 and $O_{2,heave}$ at the depth of 200m. (right column) Local regression coefficients. O_2 is regressed onto $O_{2,heave}$ and so its regression coefficients are unitless. (top) Plotted values are from the WOD13 data, (middle) from the full model output, and (bottom) from the subsampled model output.